Pramāṇa – J. Phys., Vol. 27, Nos 1 & 2, July & August 1986, pp. 193–217.

Optically selective coatings

K L CHOPRA and G B REDDY
Department of Physics, Indian Institute of Technology, New Delhi 110016

Abstract. The natural optical selectivity of a material exhibited in the form of its reflectance, transmittance, or emittance spectra can be modified and tailored to yield any desired profile by applying surface coatings in the form of multilayers of suitable materials, or composite materials having an appropriate graded composition. This paper reviews the modes of selectivity, design and modelling of some technologically important optically selective coatings.

Keywords. Optical coatings; selectivity processes; multilayer optical effects; interference stack; optical impedance matching.

PACS No. 81·15; 78·65

1. Introduction

All materials have a unique atomic lattice and corresponding electronic structure which interact dynamically with an incident electromagnetic radiation to yield a response in the form of a characteristic reflectance, transmittance, absorptance, or emittance spectra. The interaction and its variation inside the bulk of the material depend on the frequency of the radiation and the dielectric function (or optical constants) of the medium. Since the interaction depends on the radiation frequency, each material exhibits a specifically selective optical response. That is, each material exhibits a natural/intrinsic optical selectivity. Further, the interaction at the surface (interface) of the material is determined by the mismatch of optical constants across the interface. By depositing thin films/coatings of appropriate materials in the form of discrete single or multi-layers, or multicomponent composition graded layers, it is possible to alter significantly the optical spectra of a material. Such coatings which produce desired suppression or enhancement of the spectral dependence of the reflectance, transmittance, absorptance, or emittance spectra are called "optically selective coatings".

The phenomenon of modification of the optical response of a surface by means of deposited thin films/coatings has been known for over a century. However, today it is possible to precisely tailor the desired spectra by the use of sophisticated thin film technologies. As an example, figure 1 shows the reflectance profile given by the outline of the Canadian Parliament building in Ottawa. This profile can be obtained by a coating having a refractive index profile of the type also shown in the figure. Such a coating can be produced by modern thin film deposition techniques. A host of selective

---

The authors would like to dedicate this paper to Prof. D S Kothari, a great and inspiring teacher, scientist, philosopher and humanist, on the occasion of his eightieth birthday.

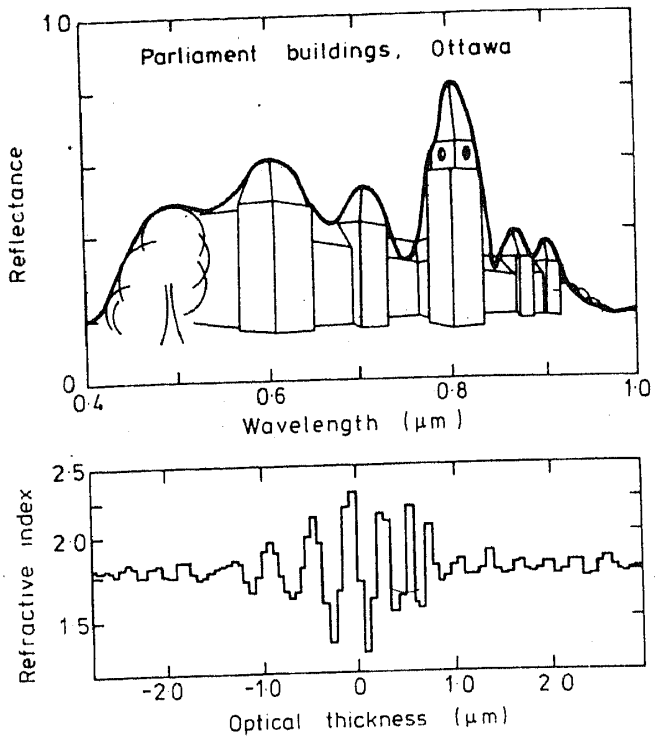

Figure 1. Filter with a spectral reflectance curve that approximates the silhouette of the Parliament Buildings, Ottawa (after Dobrowolski and Lowe 1978).

coatings have been designed and produced for such thin-film optical components as interference filters, mirrors, prisms, polarizers, gratings, switches, waveguides, lasers, emitters, solar absorbers, detectors, sensors, solar cells, display and memory devices.

The review gives a brief description of the modes of selectivity, design and modelling of some interesting optically selective coatings. The techniques for deposition of such coatings are covered extensively in literature and will not be described here. Different aspects of the present subject are covered in various books and reviews (see, for example, Macleod 1969; Chopra 1969; Heavens 1965; Chopra and Kaur 1983; Chopra *et al* 1984; Seraphin 1979).

2. Selectivity processes

2.1 *Intrinsic absorption*

As already pointed out, all materials show optical selectivity due to intrinsic absorption processes. Because of the high concentration of free electrons and presence of plasma resonance processes in metals, the metal surfaces exhibit high reflectivity in the visible and, in particular, in the infrared. Beyond the plasma resonance frequency, the metals are transparent.

In the case of semiconductors, significant absorption takes place due to band gap transitions for photons of energy greater than the band gap. The free carriers show absorption at long wavelengths. Absorption is also observed at longer wavelengths due to multiphonon and lattice vibrational modes. With increasing band gap, as in the case

of dielectrics, the band gap absorption occurs at shorter wavelengths, generally in UV and deep UV so that the dielectrics are transparent in the visible. Electronic and atomic polarization effects also contribute to absorption in the deep UV and infrared, respectively.

Figure 2 shows the reflectance/transmittance spectra of some representative metals and semiconductors. The reasonable optical selectivity shown by metals, semiconductors and dielectrics finds numerous applications in science and technology. But the degree of selectivity is not sufficiently high for many applications and also the spectral range for selectivity is not generally adjustable. The only materials which allow some modification of the optical spectra are the variable stoichiometry ones, such as transition metal oxides/carbides/nitrides, and which can also be doped heavily. The ability to tailor the selectivity as well as the spectral range is important in the modern sophisticated optical and optoelectronic devices. This point is best illustrated in figure 3 by the spectral profile of some ideal selective surfaces for various applications. These profiles can be achieved by selective coatings deposited on appropriate substrate materials.

2.2 *Multilayer optical effects*

Tandem layers/stacks: The intrinsic absorption properties of different materials can be exploited together by arranging these materials in tandem coatings. For solar thermal energy conversion applications, for example, a tandem structure consists of a visible absorber (generally low band gap semiconductors, and a number of transition metal oxides, nitrides, carbides, selenides and sulphides) and an infrared reflector (typically a metal). The absorber range has to be sufficiently thick to absorb the visible but sufficiently thin to allow long wavelength photons to reach the reflector. Due to the high refractive index of the semiconductor films, such tandem structures suffer from high reflection losses. This problem can be overcome by providing either another layer acting as antireflection coating, or a graded optical constant coating to provide optical

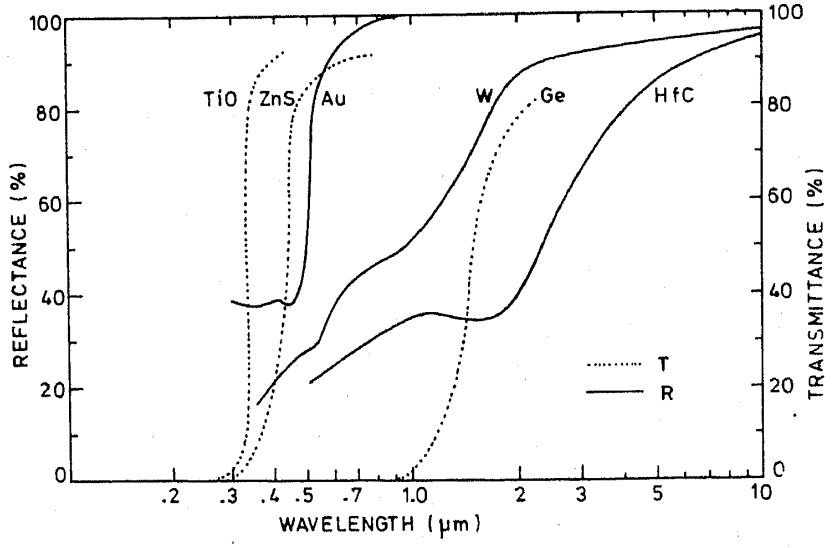

Figure 2. Spectral reflectance behaviour of polished metal surfaces of different metals and transmittance profiles of some semiconductors showing intrinsic selectivity.

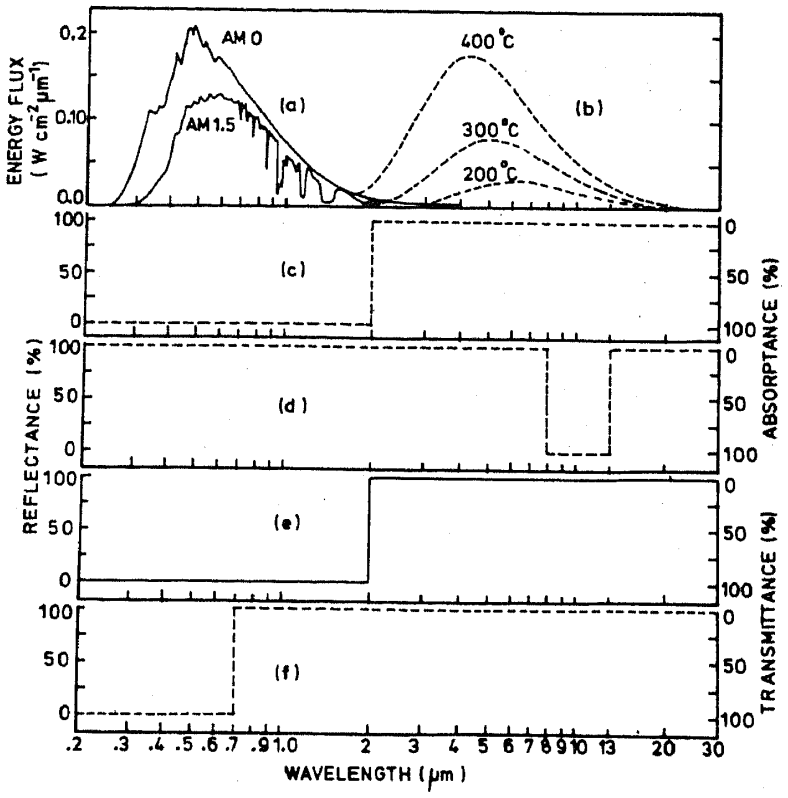

Figure 3. Spectral distribution of solar flux and reflectance profiles of different ideal selective surfaces: (**a**) solar flux outside the earth's atmosphere (AM0) and that received on earth's surface at an angle 45° (AM 1·5), (**b**) spectral distribution of the emission spectra of blackbody at 200, 300 and 400°C, (**c**) ideal solar absorber, (**d**) ideal radiative cooling surface, (**e**) and (**f**) heat mirrors.

impedance match with the ambient. Further, to arrest some unwanted processes such as oxidation of the absorber layer, or interdiffusion between the layers, it is necessary to add more coatings of appropriate material.

One may employ a tandem in reverse order, that is, with an IR reflector (or high visible transmission) followed by a visible absorber. Such a tandem (for example, a transparent conducting oxide coating on silicon) exhibits high solar selective absorption with very low emissivity in infrared.

2.3 *Interference stack*

Multiple reflections at interfaces in multilayer coatings of appropriate optical thicknesses can be utilized very effectively to obtain interference maxima or minima at any desired wavelength or a region of wavelengths. A single coating (called antireflection coating) can thus decrease the reflectance from any surface to zero at a given wavelength. With increasing number of coatings and consequently the number of interfaces, the interference conditions become more involved and allow more possibilities for tailoring the reflectance/transmittance profile of a surface to very precise values both in the degree of selectivity and the wavelength at which selectivity is desired.

Highly selective absorption properties are also possible by using a thin semi-

transparent layer between the interference stack of dielectric layers, as for example: Al_2O_3-Mo-Al_2O_3 layers (Peterson and Ramsey 1975).

Diffraction from metallic meshes and grids of appropriate geometry can be used to obtain selectivity in optical spectrum. The reflectance of a grid structure with grids of diameter a and interspacing of g is given by (Dobrowolski 1978):

$$R_\lambda = \left(\frac{2g}{\lambda} \ln \frac{g}{2\pi a} \right)^2. \tag{1}$$

Such micrometric grid structures are fabricated by microlithography techniques (Horwitz 1974).

2.4 *Optical impedance matching*

Graded index coatings: The abrupt changes in the optical impedance across interfaces in a multilayer system consisting of discrete layers of different materials result in undesirable reflectance/transmittance losses. By grading the optical constants at the interfaces to match with each other, these losses can in principle be eliminated. In the case of a multilayer interference stack, periodic grading with matched interfaces results in considerable improvements in the selectivity. As discussed later, graded index films play a major role in the performance of various solar selective black metal coatings.

Grading of optical constants is possible only by varying the composition of a film consisting of a mixture of two or more components of different optical constants. Alternatively, the grading is obtained by depositing ultrathin (a fraction of the wavelength of light to be used) layers of two or more materials with suitably varying thicknesses (see Yadava *et al* 1974).

2.5 *Resonant scattering*

By mixing two or more materials, the combined optical absorption properties of the constituents in the composite coating can be realized. If the composite coating consists of extremely fine (much less than the wavelength of light in use) particles embedded in a matrix of another material, resonant scattering between the particles plays a significant role in absorption processes. The size of the particles and the interparticle separation determine the optical selectivity properties of such composite or particulate coatings.

2.6 *Geometrical trapping*

By providing a columnar or textured structure on the coatings, multiple reflections of photons of appropriate wavelength result in the trapping of photons and hence high absorption. The selectivity of this effect depends on the dimensions of the trapping centres. If the geometry of the trapping centres can be changed along the thickness of the coating, a graded index is also obtained and can be utilized to modify selectivity.

2.7 *Quantum size effects*

Ultrathin films and nanometric particles in composite coatings may exhibit significant size dependence of the optical constants due to the effect of quantization on the plasma resonance edge, and surface plasmas. Such effects are of academic interest though these

have been used to obtain excellent selective absorbers by depositing very thin films of Ag and InSb on Al substrates (Machini and Quercia 1975).

3. Design and modelling of selective coatings

Optically selective coatings for sophisticated device applications must be tailored and tuned very precisely to utilize every incident photon. This is possible only if various absorption processes are effectively exploited in homogeneous and inhomogeneous multilayer coatings. Because of the complexities of techniques for depositing such coatings, it is essential to design and calculate the expected performance of such coatings before these are deposited. Some basic aspects of this procedure are given in this section for homogeneous as well as inhomogeneous multilayers. In the latter case, it is necessary to first calculate the equivalent optical constants by using an effective medium theory. The inhomogeneous layer can be considered as a multilayer consisting of thin homogeneous layers so that the multilayer analysis can be applied.

3.1 *Multilayer coatings*

A number of simple and sophisticated designing techniques are available in literature (Dobrowolski 1965; Macleod 1969; Seeley *et al* 1973; Liddell 1981). These can be classified into two groups: analytical and numerical. In analytical techniques, the construction parameters (refractive indices and thicknesses) are known and one calculates the spectral characteristics of the multilayer with different combinations of materials. In the case of numerical techniques, the required spectral profile being known the function of the designing technique is to find out the construction parameters.

3.1a *Analytical techniques*: The method of calculating R and T of a multilayer system with known optical constants and thicknesses is based on a matrix multiplication method (Macleod 1969). Each thin film of thickness d and refractive index n can be represented mathematically by a 2×2 matrix, derived from Maxwell's equations. The characteristic matrix of jth layer is

$$M_j = \begin{bmatrix} \cos \delta_j & \dfrac{i}{u_j} \sin \delta_j \\ i u_j \sin \delta_j & \cos \delta_j \end{bmatrix}, \tag{2}$$

where $\delta = (2\pi/\lambda)\, n_j(\text{opt})$, the quantity $n_j(\text{opt}) = n_j d_j \cos \phi_j$ is the optical thickness of the jth film, for an angle of refraction ϕ_j. The thickness mentioned in this section refers to optical thickness unless specified otherwise; u_j is the effective refractive index given by

$$u_j = n_j/\cos \phi_j, \text{ for parallel polarization,}$$

$$u_j = n_j \cos \phi_j, \text{ for perpendicular polarization.}$$

For the sake of simplification we consider an unpolarized incident beam in which case, u_j will be equivalent to n_j and u_j can be replaced with n_j in (2).

Let us consider a thin film system consisting of l layers of different materials with refractive indices of n_{1-l} and thicknesses of d_{1-l}. The construction parameters are the n's and d's of the layers and the refractive indices of substrate (n_s) and incident medium (n_0). The angle of incident and wavelength of the beam are outside parameters. The characteristic matrix of such a system is the product of l matrices representing those layers and M_s (2×1) matrix representing substrate and medium. It is given by

$$M = \prod_{j=1}^{l} M_j \times M_s. \tag{3}$$

In (2) the refractive index n of any absorbing layer ($k \neq 0$) in the system must be replaced by its complex refractive index $\bar{n}(= n - ik)$. The final matrix of a system of any number of layers is a 2×1 matrix with m_{11} and m_{21} elements and is given by

$$M = \begin{bmatrix} m_{11} \\ m_{21} \end{bmatrix}. \tag{4}$$

The specular reflectance and transmittance of such a system are given by

$$R = \left(\frac{n_0 m_{11} - m_{21}}{n_0 m_{11} + m_{21}}\right)\left(\frac{n_0 m_{11} - m_{21}}{n_0 m_{11} + m_{21}}\right)^*, \tag{5}$$

and

$$T = \frac{4 n_s n_0}{(n_0 m_{11} + m_{21})\,(n_0 m_{11} + m_{21})^*}. \tag{6}$$

Here, the star denotes the complex conjugate of the bracketed value. Thus, it is possible to obtain R and T of a multilayer system using matrix multiplication method.

According to (2), $\delta = 2\pi n_{\text{opt}}/\lambda$ for any layer. Let us consider a layer having n_{opt} values of $\lambda/2$, λ, $3\lambda/2$, ... $n\lambda/2$ so that $\cos\delta = \pm 1$ and $\sin\delta = 0$. It means characteristic matrix of a such layer will be a unity matrix. When all layers have optical thicknesses equivalent to the half wavelength or integral multiple thereof, the system will have a unity characteristic matrix. Such layers are important since the unity matrix has no effect on the R values, as if the layers were completely absent. These layers are also referred to as absent layers.

Another interesting case is, when the thicknesses are equivalent to quarter of a wavelength, or an integral multiple of it. In that case, the matrix is

$$M = \begin{bmatrix} 0 & i/n \\ in & 0 \end{bmatrix}. \tag{7}$$

This is not quite as simple as the half wavelength case but the matrix is still easy to handle for calculations. It is, of course, simpler if the material is non-absorbing ($k = 0$) dielectric material. Because of the simplicity of assemblies involving quarter-half wave optical thicknesses, designs are often specified in terms of fractions of quarter waves at a reference wavelength.

Generally, only two materials are involved in designs in a periodic manner and a convenient short-hand notation for quarter wave optical thicknesses are H and L. H refers to the higher and L to the lower refractive index material. The most generalized representation of the complete periodic multilayer is:

$$HLHL \ldots\ldots\ldots HL = (HL)^N, \tag{8}$$

where N stands for the number of times the basic structure HL gets repeated. The half-wave thick layers can also be represented in terms of quarter waves. Two consecutive HH means the half-wave layer of H material.

The optimum structures can be put into three categories:

(i) Periodic systems, where periodicity exists and the matching layers on both sides of the main system do not disturb the periodicity;

(ii) Non-periodic systems which are aperiodic because of the use of different materials for different layers randomly, or with varying thicknesses and order.

(iii) Two-material systems, deposited with a systematically varying graded index profile.

3.1b *Numerical techniques*: The basic aim of these techniques is to find out the construction parameters like the optical constants of each layer, and the number of layers of a system, which yield the required profile of reflectance or transmittance. All these techniques are based on the merit function concept, which can be defined in several ways. In one definition, it is the rms value of the differences between the desired and the present reflectance/transmittance of the system at a number of wavelengths. If a multilayer configuration can be found whose performance is a reasonable approximation to that required, one can improve it by making small changes in some or all of the construction parameters. Such a process is called "refinement" (Baumeister 1958) and the techniques used are known as "refinement techniques". The success of these refining techniques depends on the suitability of the starting configuration.

Several other techniques are available in which the starting system need not be known. These techniques are described in the following.

(i) *Exhaustive search method* (*Dobrowolski* 1965): Let us assume that the solution of our problem is a system with a number of layers around L and the refractive indices or thicknesses are not known initially. Consider then a multilayer system of L layers in which both the refractive index and thickness of each layer are allowed to assume N different values. There are N^2 different combinations of index and thickness for each layer and there will be N^{2L} different ways of choosing all the layers of the system. By calculating the merit function for all those combinations, by selecting the one with the lowest value and by refining system, we can arrive at a suitable solution.

(ii) *Gradual evolution technique* (*Dobrowolski* 1965): This technique is similar to the exhaustive search method, but the search is carried out in a step-by-step process. First, we assume the solution is possible with less number of layers (compared to the actual number) and find the best minimum of the merit function. In the second step, we take the previous solution (whole system) as a single layer on the substrate and then optimize the system to bring the merit function value to the lower side. In the next step, the present solution can be treated as the base layer. In this way we can approach the final solution in steps.

(iii) *Substructive method* (*Dobrowolski* 1973): This method is based on the use of minus filters, which are multilayer filters with essentially unit transmittance everywhere except in the rejection region. The computer program verifies the specified transmission curve and selects automatically the positions of rejection and width of the various minus filters that must be placed in series to obtain the final curve.

(iv) *Fourier transform method*: Using this method, the refractive index profile of an inhomogeneous layer having the required spectral transmittance/reflectance curve is evaluated. This inhomogeneous layer is approximated by a large number of homogeneous films. The index profile corresponding to the reflectance profile in figure 1 has been obtained by this method.

3.2 *Composite coatings*

Various effective medium theories (EMTs) (see, Maxwell Garnett 1904; Bruggeman 1935; Ping Sheng 1980a, b and Hanai 1960) have been developed to calculate equivalent optical constants of inhomogeneous composite materials.

Two-component (A and B) inhomogeneous materials of practical interest have four types of microstructure, as shown in figure 4. In the first, separated grains of A are dispersed in a continuous host of B. The second is an aggregate structure with a space-

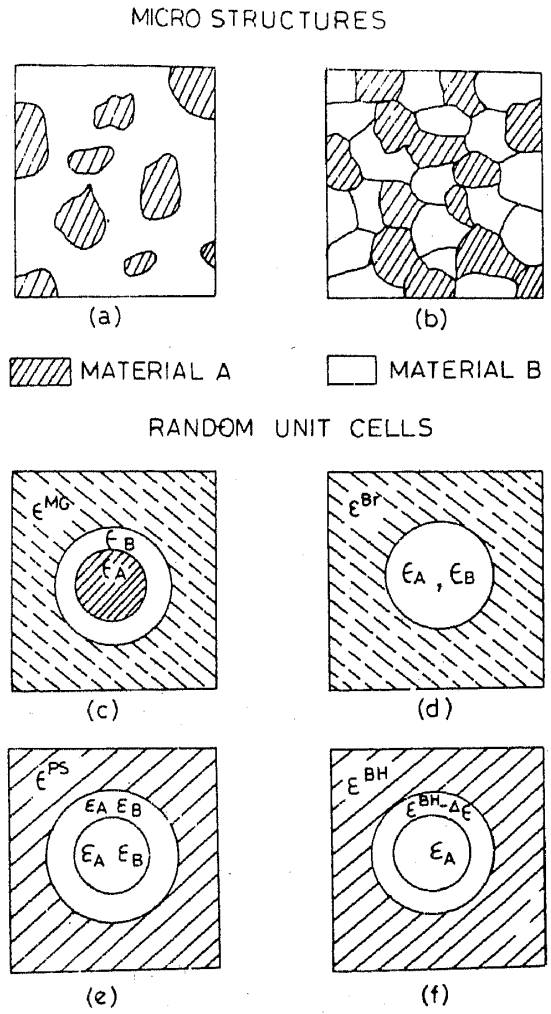

Figure 4. Schematic diagrams of the microstructure and corresponding unit cells of inhomogeneous two-phase systems composed of two materials, A and B. (**a**) and (**b**) respectively show the microstructure where A is surrounded by B and where A and B are distributed randomly. (**e**) and (**f**) show the random unit cells for the modified models of Ping Sheng and Bruggeman-Hanai theory (Niklasson 1982).

filling random mixture of the two constituents. The separate grain structures can be represented by a random unit cell being a coated sphere consisting of a core with dielectric permeability ε_A surrounded by a shell with permeability ε_B. The volume ratio of the concentric sphere is chosen so as to correspond with the overall filling factor of the inhomogeneous material. This random unit cell forms the basis of the Maxwell Garnett (MG) theory.

The aggregate structure corresponds to a random unit cell with structural equivalence of the two constituents. Therefore, this cell is taken to be a sphere whose dielectric permeability is ε_A with probability f and ε_B with probability $(1-f)$. This random unit cell leads to the Bruggeman theory.

The coated sphere microstructure (MG theory) may show spatial variation of the ratio of two materials. In some regions material A may be covered with B and in other places B material is completely covered by A as shown in figure 4a. The effective dielectric constant of such a system has been derived by Ping Sheng (1980a, b).

If the material A is covered with a shell, whose dielectric constant is influenced by the core material, the microstructure is intermediate to that of MG and Bruggeman theories. The theoretical expression for such a system has been obtained by Hanai (1960).

An effective medium may be defined as that in which the embedded random unit cell should not be detectable with an experiment using electromagnetic radiation confined to a specified wavelength range. In other words, the extinction of the random unit cell should be the same as if it were replaced with a material with the effective dielectric permeability. The extinction C_{ext}, is related to the amplitude function $S(\theta)$ by

$$C_{\text{ext}} = 4\pi \operatorname{Re}[S(\theta)/k^2], \tag{9}$$

where $k = 2\pi \bar{\varepsilon}^{\frac{1}{2}}/\lambda$, $\bar{\varepsilon}$ is the effective dielectric constant of the medium and θ is the angle of scattering. For forward direction $\theta = 0°$, so that

$$C_{\text{ext}} = 4\pi \operatorname{Re}[S(0)/k^2]. \tag{10}$$

From the definition of an effective medium, it follows that

$$C_{\text{ext}} = 0, \text{ so that } S(0) = 0,$$

which states the fundamental property of an effective medium. Fresnel's equations the apply at the boundaries of the effective medium. The derivation of the expression fc dielectric constant in the above mentioned theories has been done in the same way. Th is, the forward scattering amplitude function, $S(0)$, for different unit cells has bee obtained and equated to zero.

3.2a *Maxwell Garnett theory*

Guttler (1952) developed a series of approximation for the scattering coefficient of t coated sphere (CS) by expanding the Bessel functions in power of their arguments. T assumption in this derivation is that both the dielectric constants (ε_A and ε_B) and t particle dimensions are sufficiently small so that these series can be terminated af one or two terms. The scattering amplitude function for coated sphere is given b

$$S(0)^{\text{CS}} = i(kb)^3 p_1 + O(kb)^5 + \ldots, \tag{1}$$

where
$$p_1 = \frac{(\varepsilon_B - \varepsilon^{MG})(\varepsilon_A + 2\varepsilon_B) + f_A(2\varepsilon_B + \varepsilon^{MG})(\varepsilon_A - \varepsilon_B)}{(\varepsilon_B + 2\varepsilon^{MG})(\varepsilon_A + 2\varepsilon_B) + f_A(2\varepsilon_B - 2\varepsilon^{MG})(\varepsilon_A - \varepsilon_B)}, \tag{12}$$

$f_A = (a/b)^3$ where a is the radius of the inner sphere in the random unit cell and b is that of complete sphere. The accuracy of calculated values depends on the number of terms in (11). The higher order terms in (11) can be replaced by a quantity δ^{MG} which is a measure of the accuracy. As an example, if the δ^{MG} value is of the order of 0·015, the corresponding error in ε^{MG} would be $\sim 10\%$. So, by neglecting the higher order terms in (11), we get $p_1 = 0$. Therefore,

$$\frac{(\varepsilon_B - \varepsilon^{MG})(\varepsilon + 2\varepsilon_B) + f_A(2\varepsilon_B + \varepsilon^{MG})(\varepsilon_A - \varepsilon_B)}{(\varepsilon_B + 2\varepsilon^{MG})(\varepsilon_A + 2\varepsilon_B) + f_A(2\varepsilon_B - 2\varepsilon^{MG})(\varepsilon_A - \varepsilon_B)} = 0, \tag{13}$$

which yields

$$\frac{\varepsilon^{MG} - \varepsilon_B}{\varepsilon^{MG} + 2\varepsilon_B} = f_A \frac{\varepsilon_A - \varepsilon_B}{\varepsilon_A + 2\varepsilon_B}.$$

For ε^{MG}, we get

$$\varepsilon^{MG} = \varepsilon_B \frac{\varepsilon_A + 2\varepsilon_B + f_A(\varepsilon_A - \varepsilon_B)}{\varepsilon_A + 2\varepsilon_B - f_A(\varepsilon_A - \varepsilon_B)}. \tag{14}$$

An analogous formula for the inverted structures can be obtained by interchanging A and B in the above equation.

3.2b *Bruggeman theory*

The random unit cell in this case being a heterogeneous sphere (HS), the forward scattering ($\theta = 0$) amplitude can be written as a series

$$S(0)^{HS} = i(kb)^3 \frac{(\varepsilon - \varepsilon^{Br})}{(\varepsilon + 2\varepsilon^{Br})} + O(kb)^5. \tag{15}$$

We can replace ε with ε_A or ε_B with corresponding fill factors. Again considering small metallic sphere particles and by replacing the higher order terms we get

$$S(0)^{HS} = i(kb)^3 \frac{(\varepsilon - \varepsilon^{Br})}{(\varepsilon + \varepsilon^{Br})} + \delta^{Br}. \tag{16}$$

From the definition of the EMT $S(0)^{HS} = 0$. So we have (neglecting δ^{Br}),

$$\frac{\varepsilon - \varepsilon^{Br}}{\varepsilon + 2\varepsilon^{Br}} = 0, \tag{17}$$

and

$$f_A \frac{(\varepsilon_A - \varepsilon^{Br})}{(\varepsilon_A + 2\varepsilon^{Br})} + (1 - f_A) \frac{(\varepsilon_B - \varepsilon^{Br})}{(\varepsilon_B + 2\varepsilon^{Br})} = 0. \tag{18}$$

This equation yields the effective dielectric constant for a binary mixture.

3.2c *Ping Sheng theory*

This theory is a symmetrical generalization of the MG theory and takes account of pair-cluster interactions. In this, the coating material A is surrounded by material B at some places and at other places it is the reverse. The relative occurrence of these two types of random unit cells was determined by Ping Sheng by computing the number of equally possible configurations corresponding to different positions of the inner sphere in the random unit cell. For a sphere of material A surrounded by a shell of material B, this number V_1 is given by

$$V_1 = (1 - f_A^{1/3})^3. \tag{19}$$

For the reverse case,

$$V_2 = (1 - (1-f)^{1/3})^3 \tag{20}$$

is obtained. Taking the small sphere limit as in case of the MG theory, we get

$$V_1 \frac{(\varepsilon_B - \varepsilon^{PS})(\varepsilon_A + 2\varepsilon_B) + f_A(2\varepsilon_B + \varepsilon^{PS})(\varepsilon_A - \varepsilon_B)}{(\varepsilon_B + 2\varepsilon^{PS})(\varepsilon_A + 2\varepsilon_B) + 2f_A(\varepsilon_B - \varepsilon^{PS})(\varepsilon_A - \varepsilon_B)}$$

$$+ V_2 \frac{(\varepsilon_A - \varepsilon^{PS})(\varepsilon_B + 2\varepsilon_A) + (1-f_A)(2\varepsilon_A + \varepsilon^{PS})(\varepsilon_B - \varepsilon_A)}{(\varepsilon_A + 2\varepsilon^{PS})(\varepsilon_B + 2\varepsilon_A) + 2(1-f_A)(\varepsilon_A - \varepsilon^{PS})(\varepsilon_B - \varepsilon_A)} = 0. \tag{21}$$

Clearly, this theory yields the Maxwell Garnett result when f approaches 0 and 1.

3.2d *Bruggeman-Hanai theory*

This theory is applicable for a system having a microstructure intermediate between that of the Bruggeman and MG cases. From (11), we obtain

$$\Delta\varepsilon(\varepsilon_A + 2\varepsilon^{BH} - 2\Delta\varepsilon) + f^*(3\varepsilon^{BH} - 2\Delta\varepsilon)(\varepsilon_A - \varepsilon^{BH} + \Delta\varepsilon) = 0, \tag{22}$$

where f^* is the ratio of the volume of the inner sphere to the whole random unit cell. The filling factor of the cell f_A and that of the shell is $(f_A - \Delta f)$. Here $\Delta\varepsilon$ and Δf are the contributions to the shell due to the influence of the core cell. Thus we obtain

$$f_A = (f_A - \Delta f)(1 - f^*) + f^*, \tag{23}$$

which is equivalent to

$$f^* = \Delta f/(1 - f_A + \Delta f).$$

By replacing f^* in (22) and integrating it, we obtain

$$\frac{(\varepsilon_A - \varepsilon^{BH})}{(\varepsilon_A - \varepsilon_B)} = (1 - f_A)(\varepsilon^{BH}/\varepsilon_B)^{\frac{1}{3}}. \tag{24}$$

4. Some applications

A variety of optically selective surfaces with stringent specifications have been fabricated for different applications (Chopra and Kaur 1983; Chopra *et al* 1984; and Macleod 1969). Some useful applications of selective surfaces are described in the following.

4.1 *Photothermal conversion*

The emission spectrum of the sun outside the earth's atmosphere (called AM0) shown in figure 3(a) corresponds approximately to that of a blackbody emitting at 5600 K. The atmosphere of the earth modifies this AM0 solar spectrum significantly due to the presence of absorption bands of water vapour, carbon dioxide and ozone. The extent of modification (absorption) is a function of the angle at which radiation is received at earth's surface. For example, the AM0 1·5 solar spectrum incident on the surface of the earth at an angle 45° is shown in figure 3(a). If we compare the spectral distribution of the sun energy with that of a blackbody at 200, 300, 400°C (figure 3(b)), we note very little overlap between the solar spectrum (confined to 0·3 to 2·5 μm range) and that emitted by a blackbody at lower temperatures. Keeping this in mind, an ideal selective absorber for photothermal conversion (figure 3(c)) should have 100% absorptance in the 0·3–2·5 μm range and 100% reflectance (zero emittance) beyond 2·5 μm. Under conditions of thermodynamical equilibrium, the emittance (ε_λ) and absorptance (A_λ) are equal at a given wavelength (λ). This is, $\varepsilon_\lambda = A_\lambda = 1 - R_\lambda$ (for opaque bodies), which is the well-known Kirchoff's law. The photothermal conversion efficiency depends mainly on two parameters; solar absorptance (α) and hemispherical emittance (ε). The solar absorptance (α) of a surface/coating is given by the ratio of the absorbed energy flux to that of incident solar energy flux. The hemispherical emittance (ε) is defined as the ratio of the energy radiated per unit area at a given temperature to that radiated by the unit area of a blackbody surface at the same temperature.

A large number of solar selective absorbers based on one or more of the several physical processes described earlier have been reported in literature. Among the well known and commercially exploited coatings are: black chrome, black copper and Ni-pigmented anodized aluminium.

4.1a *Black chrome*: Electroplated black chrome (Lampert 1978, 1979; Gogna and Chopra 1979a, b) with $\alpha = 0{\cdot}98$ and $\varepsilon = 0{\cdot}08$ is a composite coating of Cr and Cr_2O_3. It consists of three regions: (i) a thin Cr_2O_3 top layer, (ii) an intermediate Cr_2O_3-Cr cermet; and (iii) a Cr rich Cr-Cr_2O_3 cermet dominated by Cr and Ni substrate. An Auger depth profile of the coating shown in figure 5 provides a direct evidence for the proposed structure. The top Cr_2O_3 layer acts as an optical impedance matching layer to minimize reflection losses. Absorption takes place in the intermediate cermet layer by the resonant scattering process. These two layers are transparent to IR radiations so that the lower metal-rich layer and particularly the substrate give rise to high IR reflectivity. The reflectance of such a coating is shown in figure 5a.

4.1b *Black copper*: Black copper selective absorbers developed in our laboratory (Kumar *et al* 1986) are the best example, where surface texturing, optical matching and metal/semiconductor tandem effects contribute to yield high selectivity ($\alpha = 0{\cdot}98$, $\varepsilon = 0{\cdot}14$). By adjusting the chemical conversion parameters, copper oxide coatings with

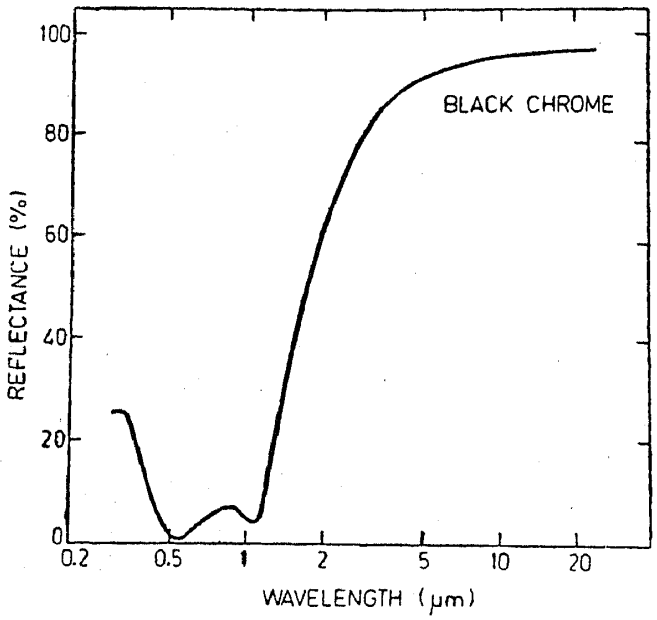

(a)

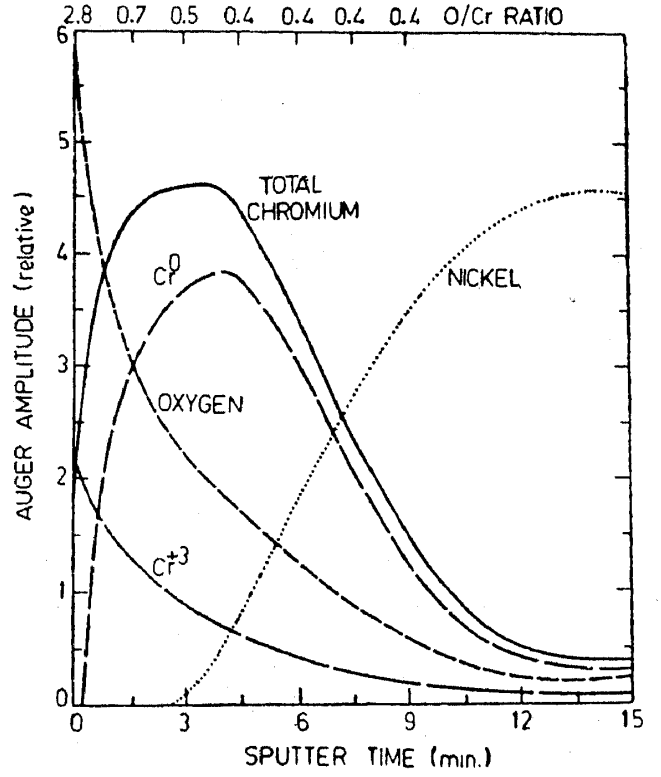

(b)

Figure 5. a. Total reflectance spectrum of electroplated black chrome on nickel plated copper. **b.** Auger depth profile of the above coating showing the variation of total chromium, free metallic chromium, Cr^0, chromium in Cr_2O_3 as Cr^{+3} and oxygen. Scale at the top shows the variation of oxygen-to-chromium ratio. The onset of nickel signal indicates the beginning of substrate interface (Lampert 1978).

a fine columnar-structured surface topography, have been obtained. The major part of the absorption occurs in Cu_2O film during double passage of light. The emittance is determined by the Cu substrate. About 8 % absorption is due to the surface texturing

which is indicated by the difference between the measured total and specular reflectance values (figure 6). Further, a thin CuO layer on the surface provides optical matching at the interface.

4.1c *Metal pigmented anodized aluminium selective surfaces*: The Ni/Co/Zn, pigmented aluminium selective absorbers (Granqvist *et al* 1979; Kumar *et al* 1983) with $\alpha = 0{\cdot}94$ and $\varepsilon = 0{\cdot}10$ have been fabricated using an anodization process for producing porous cylindrical columns of alumina and subsequently filling a part of the columns with a metal by electrodeposition. The cross-section of the coating, shown in figure 7a, consists of four layers: (i) porous Al_2O_3 layer (grooves opening part); (ii) porous Al_2O_3 layer (cylindrical porous); (iii) Ni pigmented Al_2O_3 composite and (iv) Al_2O_3 barrier layer, on the aluminium substrate. To understand the absorption process, Granqvist *et al* (1979) have calculated reflectance values of individual layers and combinations of the layers (see figures 7b, c) using matrix multiplication method described earlier. The effective optical constants of each layer have been calculated using Maxwell Garnett theory (figure 7b) and Bruggeman theory (figure 7c). The top two layers are assumed to be composite layers of Al_2O_3 and air. This system shows a fair selectivity with λ_c at 1·2 μm for the MG model and at 5 μm for the Bruggeman model. A comparison with the experimental data shows that the Bruggeman theory gives a better description of the measured data. The calculated reflectance profile of Ni pigmented layer (layer 3) clearly shows high reflection ($\sim$ 12%) losses, which has been substantially reduced with the addition of the top two optically matching layers. The high selective absorption is clearly due to the graded index structure of the coatings.

4.2 *Hear mirrors*

Selective coatings (figures 3(e) and 3(f)) which allow the transmission of the visible and reflection of the IR from the solar spectrum are called heat mirrors. Such coatings are of

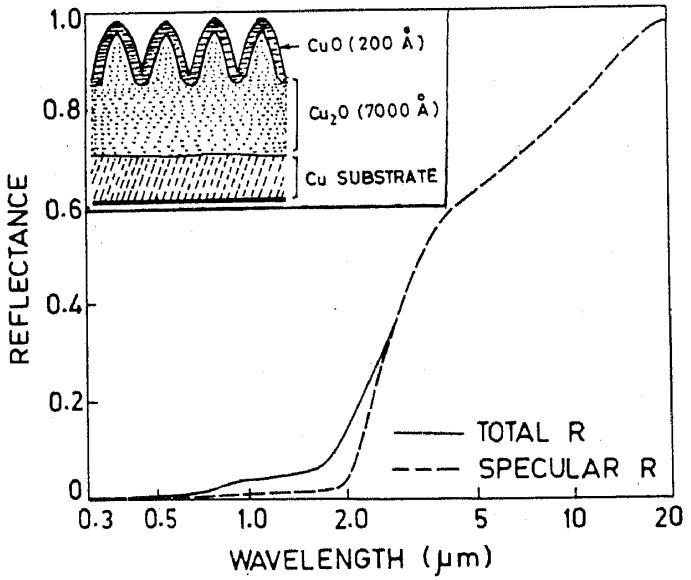

Figure 6. Total and specular (5°) reflectance profiles of chemically converted black copper selective absorber. Schematic cross-section of the coating is shown in inset (Kumar *et al* 1986).

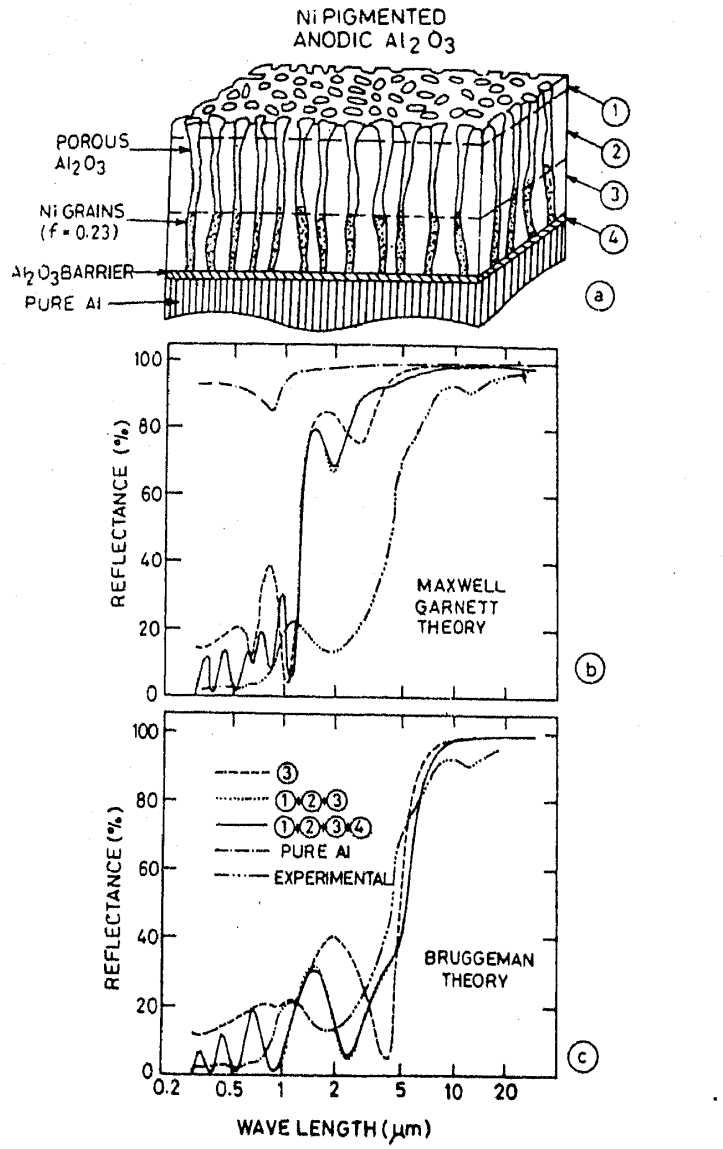

Figure 7. **a.** Four-layer structure model for Ni pigmented anodic Al_2O_3 containing 0·62 g Ni per m^3. Filling factor for layer 3 is 0·23, (**b**) and (**c**) show reflectance behaviour as calculated for individual layers and combination of layers by using Maxwell Garnett and Bruggeman theories, respectively. Experimentally measured reflectance curve has been added for comparison with theory (Granqvist *et al* 1979).

considerable interest in controlling the temperature of closed spaces with windows in buildings and of devices (such as solar cells) and instruments (e.g. in a space satellite) exposed to solar radiations. Also, these selective coatings could be used to keep the heat confined within a closed space with windows in a cold environment, or a solar collector.

The selectivity requirements for different applications are clearly different. Whereas conservation of space heating would require window materials to reflect back the far IR (beyond 2 μm) emitted from within, the conservation of space refrigeration would require window materials to reflect the near IR (above 0·7 μm) from solar radiations. The latter requirement is also applicable to solar cells. The single layer selective coatings

which may have the desirable properties are those of doped and nonstoichiometric oxides of In, Sn, Cd, Zn and their alloys. Typical reflectance and transmittance spectra of F-doped tin oxide (Shanthi *et al* 1980, 1982) are shown in figure 8. The optical spectra are dominated by the electron transport parameters, particularly due to the onset of plasma resonance. The plasma resonance edge can be shifted continuously by doping as seen in figure 8 from about one to several microns. The presently available transparent conducting oxide films are, therefore, well suited for keeping heat radiations confined in a building, but offer little advantage to keep out the heat radiations from the sun. For the latter application, it is necessary to develop new materials with reflectance edge around 0·7 μm. In a way partly transparent films of high conductivity metals (e.g. Al, Cu) provide some desirable features at the expense of reduced visible transmission. Among the promising materials which need to be further studied are ReO_3 and Na_xWO_3 (Fan *et al* 1974) and rare earth hexaborides.

4.2a *Dynamic (smart) window coatings*: A dynamic (smart) window coating is one, the transparency of which can be changed dynamically by an external variable parameter. The dynamic component is a chromogenic material in thin film form. Optical properties of chromogenic materials change drastically under the influence of light, heat, electric field or a combination. Correspondingly these materials are called photochromic, thermochromic and electrochromic. The solar transmission of such a material changes due to increased reflectance or absorptance over a part of the solar spectrum. The electrochromic materials are the most promising class of material, where the optical changes are reversible and can be modulated by an applied electric field. A number of materials, both organic and inorganic liquids and solids, exhibit this

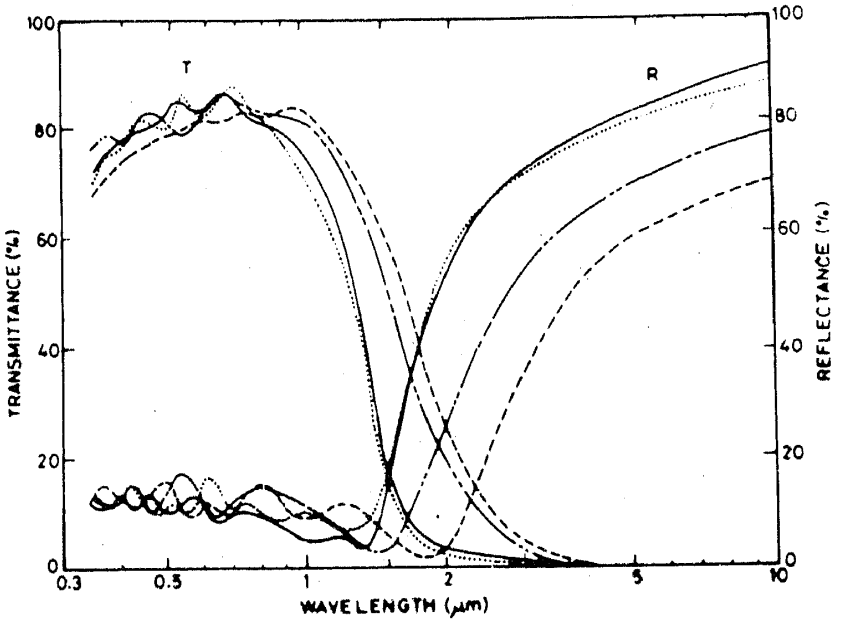

Figure 8. Transmittance T and reflectance R spectra of fluorine-doped tin oxide (FTO) films showing the shift in plasma reflection edge (λ_p) to shorter wavelengths with increasing carrier concentration (N): – – – –, $N = 2{\cdot}5 \times 10^{20}$ cm^{-3}, $\lambda_p = 2{\cdot}4$ μm; ———, $N = 3{\cdot}7 \times 10^{20}$ cm^{-3}, $\lambda_p = 1{\cdot}9$ μm; ——, $N = 4{\cdot}6 \times 10^{20}$ cm^{-3}, $\lambda_p = 1{\cdot}6$ μm; . . . . ., $N = 4{\cdot}9 \times 10^{20}$ cm^{-3}, $\lambda_p = 1{\cdot}5$ μm (Shanthi *et al* 1982).

phenomenon. Among the important materials are the oxides of tungsten and molybdenum (Lampert 1984).

The coloration of WO_3 is described by the chemical reaction (figure 9a):

$$\underset{\text{(transparent)}}{WO_y} + x\,H^+ + x\,e^- \underset{}{\overset{\text{electric field}}{\rightleftharpoons}} \underset{\text{(blue)}}{H_x\,WO_y} \tag{25}$$

That is, by driving both protons and electrons into a transparent WO_3 film, it can be converted into blue coloured $H_x\,WO_y$ material. By reversing the polarity of the driving force, we can get back the original material. The first step is called "coloration" and the second step is known as "bleaching". A generalized reaction is:

$$MO_y + xA^+ + x\,e^- \rightleftharpoons A_x\,MO_y, \tag{26}$$

where x can have values between 0 and 0·5, with y from 2·97 to 3·0, $A^+ = H^+$, Li^+, Na^+ or Ag^+. Any of the ionic conductors based on Li, Ag or Na can be used.

The basic elements of an electrochromic device (figure 9a) consist of: (i) two electrodes to inject charge carriers—these can be either transparent conductors or semitransparent metal films, (ii) an active electrochromic layer, (iii) an electrolyte or ionic conductor which may be an insulator, liquid or solid electrolyte, and is referred to as counter electrode.

Figure 9b shows the shift of the transmission edge with applied electric field for a reactively evaporated WO_3 smart window reported by Svensson and Granqvist (1985). The electrolyte is 1 M dehydrated lithium perchlorate in propylene carbonate which also acts as the counter-electrode. The two transparent conductors on both sides of the system are thin-ITO films.

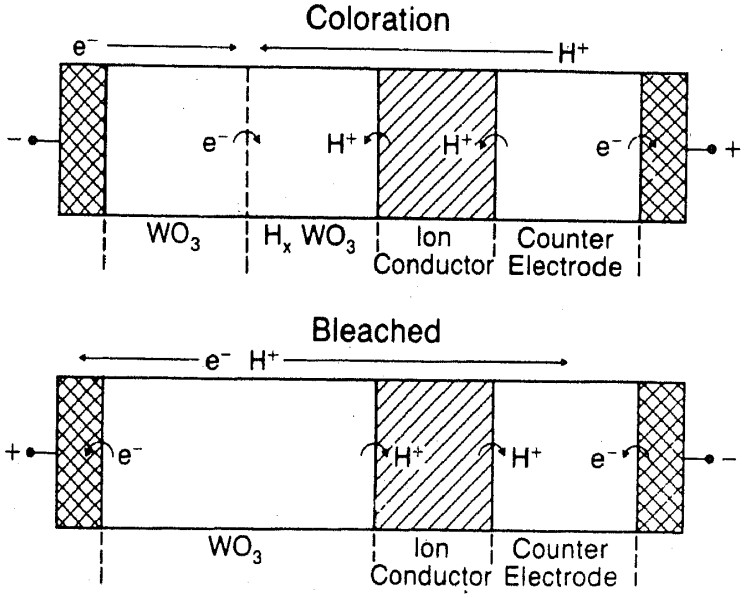

Figure 9(a). Schematic of coloration and bleaching reactions within WO_3. During coloration the reaction proceeds with injection of protons and electrons. During bleaching, protons and electrons are depleted from the H_xWO_3 layer.

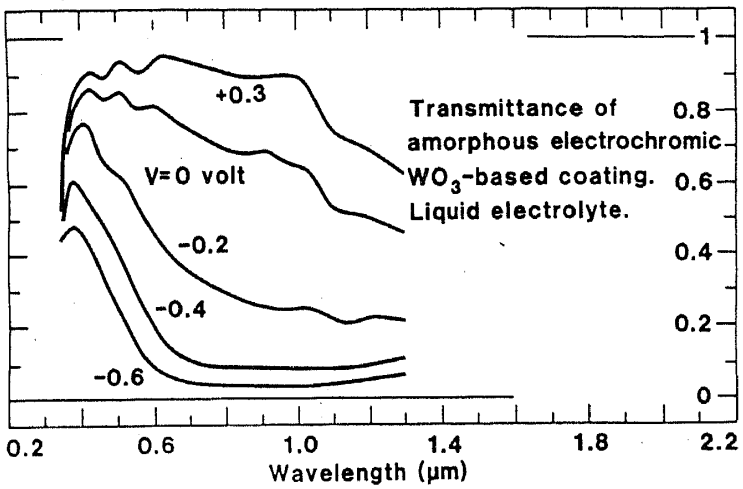

Figure 9(b). Spectral normal transmittance measured for an electrochromic WO_3-based film, on contact with a liquid Li^+-electrolyte, as a function of voltage between working and reference electrodes (Svensson and Granqvist 1985).

4.3 *Radiative (emissive) cooling*

The cooling of surfaces by radiation is a well-known phenomenon. To increase the cooling efficiency of a surface, the emittance spectra of the surface and that of the sky have to match. That is, in the 8–13 μm region where the atmosphere is transparent, the emittance of the surface has to be high so that the radiations are coupled directly to the outside atmosphere thereby increasing the cooling efficiency. The ideal spectral profile for such a surface is shown in figure 3(c).

The infrared transmittance of the sky depends on meteorological conditions and the zenith angle (Granqvist and Hjortsberg 1981). For increasing zenith angle, the atmosphere becomes gradually more like a blackbody at all wavelengths. The radiative power and temperature drop below ambient for horizontal surfaces which radiate towards the sky can be evaluated (Granqvist 1981) for model atmospheres. For a heat transfer coefficient of 1 $Wm^{-2}K^{-1}$, the maximum temperature difference for the blackbody is 11–21°C and for an IR selective surface is 18–33°C. The radiative cooling power is given by

$$P_{\text{cool}} = P_{\text{out}} - P_{\text{in}},$$
$$= \varepsilon_s \sigma (T_s^4 - T_a^4) + (1 - \varepsilon_{av})\,\varepsilon_{s2} \int_{8\mu\text{m}}^{13\mu\text{m}} W(T, \lambda)\,\mathrm{d}\lambda, \tag{27}$$

where W is the Planck function, ε_a and ε_s are the average emittances of atmosphere and the samples, respectively, ε_{s2} is the integrated emittance of the sample in 8–13 μm region. To achieve good cooling, $\eta = \varepsilon_{s2}/\varepsilon_s$ must be maximum so that the cooling power is governed by ε_{s2}. Such surfaces have been produced by evaporating SiO in the presence of nitrogen on aluminium (Granqvist 1984). Figure 10 shows the measured and theoretically calculated reflectance profile of $SiO_{0.6}N_{0.2}$ coating on aluminium (Granqvist 1984). The reflectance minimum in 8–13 μm is due to strong lattice absorption combined with destructive interference. The author has shown that using such surfaces, temperatures $\sim$ 14°C below the ambient can be obtained.

4.4 *Antireflection (AR) coatings*

Reflection losses are reduced by antireflection coatings and are thus required to enhance the efficiency of such devices as solar cells. The material chosen for an AR coating depends upon the optical properties of the outermost surface considered and the nature of the application that needs it.

Materials used in solar cells such as Si, GaAs, and CdTe have high indices of refraction and consequently have high reflection losses. For example, bare-polished silicon ($n = 3{\cdot}85$ at $\lambda = 0{\cdot}8$ μm) reflects an average 35 % of the incident solar radiation in the 0·3–1·2 μm region. An ideal AR coating should act as a perfect band pass filter (0·4–1·2 μm region) with no absorption on either side. This can be achieved by properly designed single layer or multilayer structures. The best advantage of single layer is in the case of obtaining the AR coating. For example, for Si, neglecting dispersion, a quarterwave AR layer requires a material (e.g. silicon nitride) of refractive index 1·96. The thickness d of a single layer, which gives zero reflectance at a given λ_{min} is determined by $\lambda_{min} = 4\,nd$. A quarterwave Si_3N_4 coating with λ_{min} at 0·55 μm reduces the reflectance of Si surface to an average of 12 % in 0·4–1·2 μm region. Another useful single large material is SiO with refractive index of 1·8–1·9. However, this material has some absorption losses in the visible region. Koltun (1981) reported that $\sim$ 0·15 μm layer of SiO is the optimum layer on Si solar cells under AM0 illumination. This layer produces a 45 % increase in the short circuit current J_{sc} of the cell (figure 11). It should be noted that with change in optical thickness of SiO, the position of reflectance minima changes and consequently the spectral response can be enhanced in a selected spectral region.

Single layer AR coatings have a limitation that the reflectance in the vicinity of λ_{min} increases rapidly yielding a high value of average reflectance. The reflectance can be

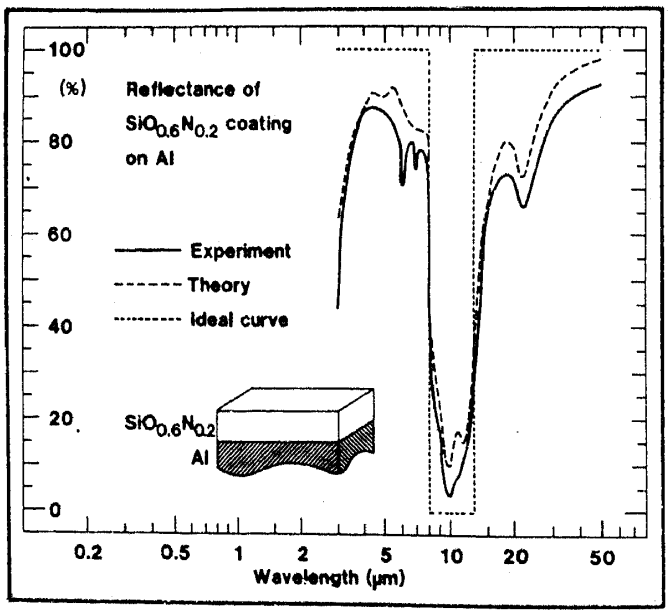

Figure 10. Spectral reflectance of a surface for radiative cooling to low temperatures by selective infrared emission. Dotted lines indicate the ideal property, solid curve represents a measurement on an Al substrate coated with 1·3 μm of $SiO_{0.6}N_{0.2}$ and dashed curve shows the results of a computation (after Granqvist 1984).

further reduced by either using a multilayer AR coating, or by texturing the surface of the cell and then depositing a single AR layer. A number of multilayer AR coatings are possible and have been studied by Koltun (1981) for silicon solar cell. Deposition of the two layer $CeO_2 + SiO_2$ or $ZnS + MgF_2$ AR coating on Si solar cell produces a 55% increase in J_{sc}. A five-layer ($TiO_2 + CeO_2 + ZnO_2 + SiO + Al_2O_3$) AR coating further improves the response of the cell.

4.5 *Optical filter*

4.5a *Band rejection filter*: Such filters can be fabricated with two dielectric materials forming a (HLH) or $(0{\cdot}5\,HL\,0{\cdot}5\,H)$ structures. The optical constants must satisfy the conditions (Macleod 1969):

$$n_s n_0 = n_H^3/n_L, \quad \text{or} \quad n_s n_0 = n_H n_L. \tag{28}$$

The maximum reflection of this filter is a function of n_0, n_s, n_H, n_L and the number of layers and is given by:

$$R_{\max} = \left[\frac{n_0/n_s - (n_H/n_L)^{2N}}{n_0/n_s + (n_H/n_L)^{2N}}\right]^2 \tag{29}$$

for quarter wave coatings. Rejection will be high for higher N-values and $R \to 1$ as $N \to \infty$.

The bandwidth is given by:

$$\frac{\Delta\lambda}{\lambda} = \frac{4}{\pi}\sin^{-1}\left(\frac{1 - n_H/n_L}{1 + n_H/n_L}\right). \tag{30}$$

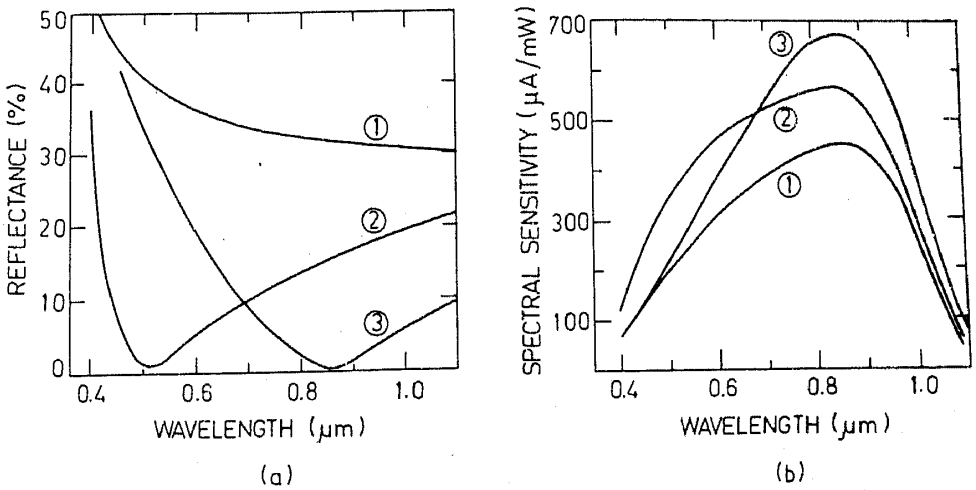

Figure 11. Wavelength dependence of (**a**) reflectance and (**b**) absolute spectral sensitivity of a silicon solar cell with an AR coating of SiO. (1) without AR coating, (2) with SiO coating of optical thickness 0·125 μm and (3) with SiO coating of optical thickness 0·2125 μm. It should be noted that with change in optical thickness of SiO, the position of reflectance minima changes and consequently the spectral sensitivity can be enhanced in selected spectral region (Koltun 1981).

As the number of layers increases, the width decreases so that the system becomes a narrow band rejector. The side peaks are reduced by choosing low values of n_H/n_L which also effects the bandwidth.

A number of band rejection filters in series forms an 'edge filter' to transmit or reject beyond a reference wavelength. Using zinc sulphide ($n_H = 2{\cdot}35$) and cryolite ($n_L = 1{\cdot}35$) material, Welford (1954) developed a longwave pass filter beyond 0·450 μm with basic structure (0·5 LH 0·5 L) repeating seven times on a glass substrate. Using the same materials by replacing H layer with the L layer and vice versa, a short wave pass filter below 0·75 μm is obtained. Thus, the same set of materials can be used to obtain different profiles depending on the order of the arrangement.

4.5b *Narrow band pass filters*: The filter is based on the principle of Fabry-Perot interferometer (Macleod 1969). The transmittance of the filter is given by

$$T = \frac{T_s}{(1-R_s)^2} \cdot \frac{1}{1+F\sin\delta}, \tag{31}$$

where $F = 4R_s/(1-R)$, $\delta = 2\pi n_s d_s \cos\theta/\lambda$, R_s, the inner surface reflectance of the plates, n_s, the refractive index of the spacer, and d_s, the thickness of the spacer. We see that T will be maximum when $\delta = m\pi$, (m is an integer) so that a series of $T_{\max}$'s of different orders will be obtained.

Figure 12 shows the measured transmittance of a very narrow-band all dielectric multilayer filter with bandwidth as 11 Å. The filter is made of ZnS and cryolite films on a glass substrate. In this case of an all dielectric Fabry-Perot interferometer, the reflector plates are replaced with a highly reflecting multilayer structures of the form $(HL)^3$. The spacer can be either H or L. So, the final structure of this system is $(HL)^3$ H spacer $(HL)^3$ or $(HL)^3$ L spacer $(HL)^3$. The bandwidth is given by

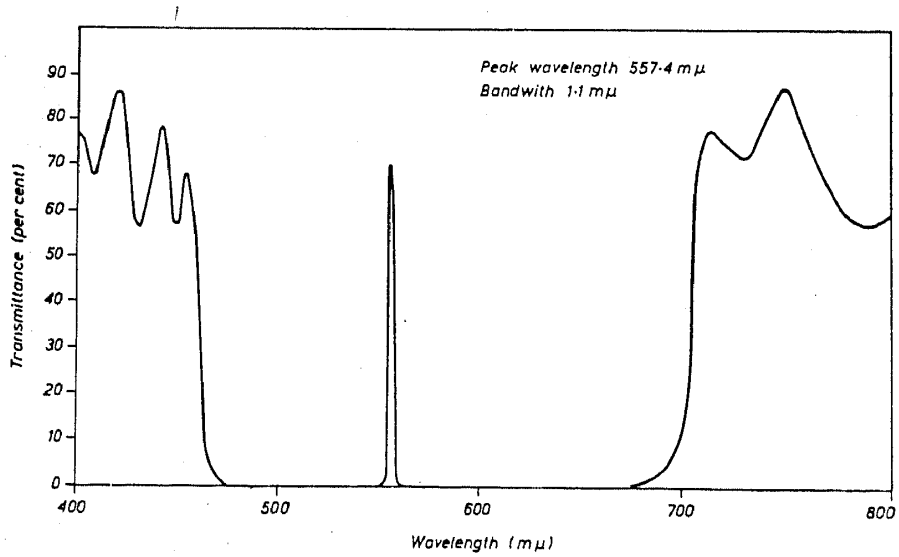

Figure 12. Measured transmittance of a narrow-band-all-dielectric filter with unsuppressed sidebands. Zinc sulphide (H layer) and cryolite (L layer) were the thin film materials used (Macleod 1969).

$$\frac{\Delta\lambda}{\lambda} = \frac{4n_s n_L^{2x}}{m\pi n_H^{2x+1}} \quad \text{with} \quad H \text{ spacer,} \tag{32}$$

$$\frac{\Delta\lambda}{\lambda} = \frac{4n_s n_L^{2x-1}}{m\pi n_H^{2x}} \quad \text{with} \quad L \text{ spacer,} \tag{33}$$

$x = 3$ is the number of H layers used in the side or reflectors. The side bands appearing on both sides (figure 12) can be suppressed by using a transmission filter in series or with the help of a metal-dielectric blocking filter. Side bands of lower wavelengths side can be removed using an appropriate glass substrate.

4.5c *Graded index multilayer filter*: By providing optical matching at the interfaces between materials forming a multilayer structure, the performance of the multilayer stack can be improved considerably. Optical matching can be achieved by using graded index films obtained by either codeposition of two or more materials with varying composition, or by depositing alternate layers of two materials of varying thicknesses (with step thickness much less than the wavelength of the light to be used) in symmetrical LHL or LHL combinations. The homogeneous layers of graded index can be further divided into a symmetrical units of three layers HLH or LHL. The refractive index of any HLH or LHL unit can be varied anywhere between the refractive index of L and that of H, by changing the relative thicknesses approximately. Figure 13a shows the measured and calculated reflectance profile of a graded (multilayer) system reported by Yadava *et al* (1974). The film exhibits much superior performance as compared to the normal $\lambda/4$ filters. The system consists of 13 units of LHL, with H (ZnS, $n = 2{\cdot}35$) and L (MgF_2, $n = 1{\cdot}37$) films. The relative thicknesses (shown in figure 13b) of these units have been chosen so that the equivalent refractive index goes through a maximum ($= 2{\cdot}35$) as shown in the same figure. The equivalent refractive index has been calculated using Clausious-Mossotti relation.

5. Concluding remarks

(i) Optical modelling techniques have now been perfected to allow the design of a surface/coating of any desired spectral reflectance, transmittance or absorptance characteristic.

(ii) The preparation of such designed selective surface is possible by using thin-film materials having specified optical constants and their spatial gradients. Thus, tailor made thin-film optical materials in the form of multilayers, superlattices and homogeneously/heterogeneously graded composites are required and can be obtained by thin-film techniques.

(iii) The dielectric function and optical behaviour of the composite structure selective coatings can be predicted by one of the several effective medium theories. The mathematical analysis in many cases is empirical in nature. A more fundamental approach to the problem based on atomic polarizability and percolation process is yet to be developed.

(iv) Selective coatings already find major applications in a number of optical and opto-electronic devices and instruments. Among the major new areas of applications in the future are: integrated optics, solar energy conversion, radiation-controlled architecture and image conversion.

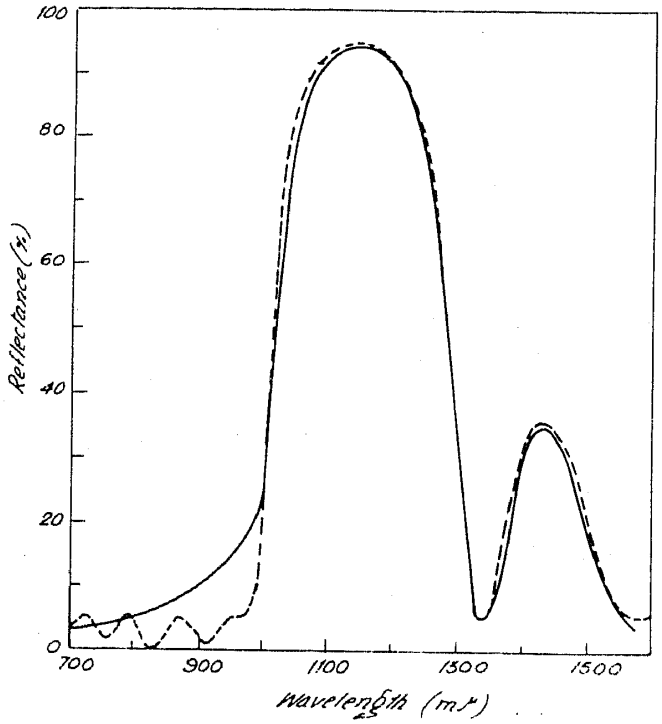

Figure 13(a). Experimental (solid line) and theoretical (broken line) reflectance curves for a graded index ZnS-MgF_2 multilayer composed of 13 basic periods.

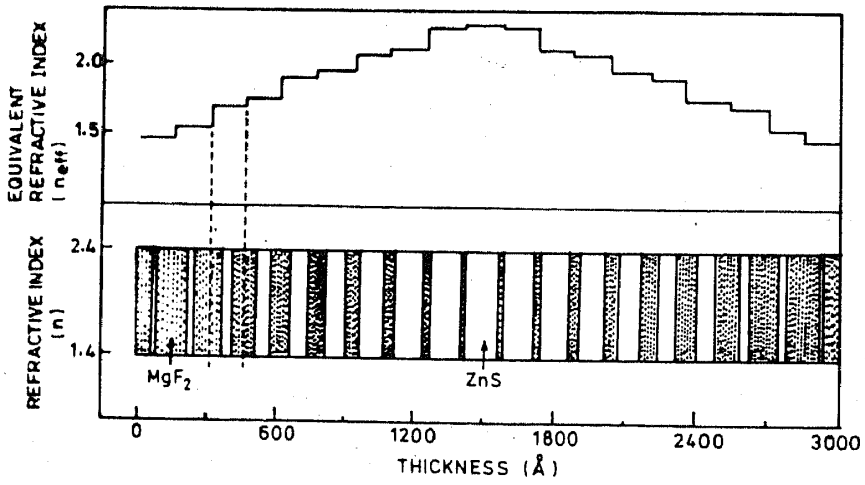

Figure 13(b). The profile of the equivalent refractive index and the relative thicknesses of *H* and *L* layers.

References

Baumeister P W 1958 *J. Opt. Soc. Am.* **48** 955
Bruggeman D A G 1935 *Ann. Phys.* **24** 636
Chopra K L 1969 *Thin film phenomena* (New York: McGraw-Hill)
Chopra K L and Kaur I 1983 *Thin film applications* (New York: Plenum Press)
Chopra K L, Major S and Pandya D K 1983 *Thin Solid Films* **102** 1
Chopra K L, Pandya D K and Malhotra L K 1984 in *Reviews of renewable energy resources* (eds) M S Sodha, S S Mathur and M A S Malik (New Delhi: Wiley Eastern Limited) Vol. 2, Ch. 3

Dobrowolski J A 1965 *Appl. Opt.* **4** 937
Dobrowolski J A 1973 *Appl. Opt.* **12** 1885
Dobrowolski J A 1978 in *Handbook of optics* (ed.) W G Driscoll (New York: McGraw-Hill) Ch. 8, p. 107
Dobrowolski J A and Lowe D 1978 *Appl. Opt.* **17** 3039
Fan J C C, Reed T B and Goodenough J B 1974 *Proc. of 9th Int. Soc. Energy Conven. Engg. Conf.*, San Francisco p. 341
Gogna P K and Chopra K L 1979a *Thin Solid Films* **57** 299
Gogna P K and Chopra K L 1979b *Sol. Energy* **23** 405
Granqvist C G 1981 *Appl. Optics* **20** 2606
Granqvist C G 1984 *Physics Teacher* p. 372 (Sept.)
Granqvist C G, Anderson A and Hunderi O 1979 *Appl. Phys. Lett.* **35** 268
Granqvist C G and Hjorstberg A 1981 *J. Appl. Phys.* **52** 4205
Guttler A 1952 *Ann. Phys.* **6** 11, 65
Hanai T 1960 *Kolloid Z.* **171** 23
Heavens O S 1965 *Optical properties of thin solid films* (New York: Dover)
Horwitz C M 1974 *Optics Commun.* **11** 210
Koltun M M 1981 *Selective optical surfaces for solar energy converters* (New York: Allerton Press)
Kumar S N, Malhotra L K and Chopra K L 1983 *Sol. Energy Mater.* **7** 439
Kumar S N, Purnima R, Malhotra L K and Chopra K L 1986 *Thin Solid Films* (To be published)
Lampert C M 1978 Ph.D. Thesis (Univ. of California, USA)
Lampert C M 1979 *Solar energy materials* **1** 319
Lampert C M 1979 *Solar energy materials*, Ph.D. Thesis (University of California) p. 319
Lampert C M 1984 *Solar Energy Mater.* **11** 1
Liddell H M 1981 *Computer-aided techniques for the design of multilayer filters* (London: Adam Higher)
Machini N A and Quercia I F 1975 in *Proc. 1st Course on solar energy conversion*, Preocide, Italy
Macleod H A 1969 *Thin film optical filters* (London: Adam Hilger)
Maxwell Garnett J C 1904 *Philos. Trans. R. Soc. (London)* **A203** 385
Niklasson G A 1982 Ph.D. Thesis, Chalmers University of Technology, Gotenberg, Sweden
Peterson R E and Ramsey J R 1975 *J. Vac. Sci. Technol.* **12** 471
Ping Sheng 1980a *Phys. Rev. Lett.* **45** 60
Ping Sheng 1980b *Phys. Rev.* **B22** 6364
Seraphin B O 1979 *Topics in applied physics* (ed.) B O Seraphin (New York: Springer-Verlag) Vol. 31
Shanthi E, Banerjee A, Dutta V and Chopra K L 1980 *J. Appl. Phys.* **51** 6243
Shanthi E, Banerjee A, Dutta V and Chopra K L 1982 *J. Appl. Phys.* **53** 1615
Sheeley J S, Liddell H M and Chen T C 1973 *Opt. Acta* **20** 641
Svensson J S E M and Granqvist C G 1985 *Thin Solid Films* **126** 31
Thornton J A, Penfold A S and Lamb L L 1980 *Thin Solid Films* **72** 101
Welford W 1954 *Vacuum* **4** 3
Yadava V N, Sharma S K and Chopra K L 1974 *Thin Solid Films* **21** 297